Załącznik II

English

SUMMARY OF ACHIEVEMENTS

Agnieszka Obłąkowska-Mucha

Contents

I. Personal data 2
II. The main scientific achievement 2
III. Description of the main scientific achievement 3
Preface 3
1. LHCb experiment 4
2. Radiation damage in the semiconductor VELO LHCb sensors 5
2.1 Monitoring of the radiation damage in the VELO sensors 7
2.2 Fluence simulation 9
3. Measurement of the Standard Model parameters 11
3.1 Potential of $B \to DX$ decays 12
3.2 CKM angle γ 12
3.3 Analysis of the $B_s^0 \to D_s^{\mp} K^{*\pm}$ decay 14
3.3.1 Branching fraction estimation 14
3.3.2 Data selection 15
3.3.3 Results from the experimental mass fits 16
3.3.4 Prospects of $B_s^0 \to D_s^{\mp} K^{*\pm}$ measurements in RUN III 18
Summary 18
References 19
IV. Description of the other scientific achievements 20
1. B Physics 20
2. Radiation damage 21
3. Teaching and popularisation of physics 21

KRAKÓW 2019

I. Personal data

Name:	Agnieszka Obłąkowska-Mucha
Email, phone	amucha@agh.edu.pl, +48 12 617 29 88, +48 606 14 14 37
Diplomas and scientific degrees:	2002 Ph.D. in physics AGH University of Science and Technology Faculty of Physics and Applied Computer Science Thesis title: The observation of $\eta_c(2980)$ through for particles decays in γγ interactions at DELPHI experiment Promotor: prof. dr hab. Bogdan Muryn 1995 Master of science and engineer degree in Technical Physics AGH University of Science and Technology Faculty of Physics and Nuclear Techniques Master thesis title: Search for a $f_2(1525)$ production in two photon interaction et LEP energies
Current employment:	AGH University of Science and Technology Faculty of Physics and Applied Computer Science Al. Mickiewicza 30 30-059 Kraków
2002-	Assistant professor
2001-2002	Assistant

II. The main scientific achievement

As a scientific achievement according to the Par. 16 Act. 2 from 14th of March 2003 Act on academic degrees and academic titles and degrees and title in art (Dz. U. 2016 r. poz. 882 ze zm. w Dz. U. z 2016 r. poz. 1311.) I indicate the monograph:

Title:	**Radiation damage in the LHCb Vertex Locator. First observation of $B_s^0 \to D_s^{\mp} K^{*\pm}$ decay**
Author:	Agnieszka Obłąkowska-Mucha
Year	2018
Publisher:	Wydział Fizyki i Informatyki Stosowanej Akademia Górniczo-Hutnicza im. Stanisława Staszica Al. Mickiewicza 30, 30-059 Kraków Wydawnictwo JAK ISBN 978-83-64506-60-4
Publisher's referee:	Dr hab. inż. Tomasz Szumlak, prof. AGH

III. Description of the main scientific achievement

Preface

The main motivation for the construction of the Large Hadron Collider (LHC) was to verify the outcomes of the Standard Model (SM). The previous experiments left us with the problem of the Higgs boson discovery and with vast of theories that need to be either confirmed of ruled out. To do this one needed to construct the apparatus that would play the role of a forerunner in the technology, computing and method of analysis.

The LHC accelerates protons[1] to energies never achieved before: $\sqrt{s}$ =7-13 TeV, luminosity is two order of magnitude higher than ever obtained, time between collisions is only 25 ns. Places of collisions are surrounded by sophisticated detectors, which aim is to catch and identify whatever was produced. The task for the scientists is to translate this information into results that would carry valuable insights into the theory. That requires huge groups of engineers and scientists to design, build and monitor the devices, and not less physicists to analyse and interpret the data.

I had an opportunity to participate in the operation of the LHCb spectrometer from the time of construction till just finished second period of the data taking (Run II). I think that the awareness how the measurement is done is necessary for the understanding the physics. During my scientific career I have undertaken various subjects that helped me to realise how the data were collected and how they could be interpreted in order to turn into valuable results. I participated in the simulation work, detector monitoring and tests of the tracking algorithms. I analysed the data with sophisticated statistical tools.

From the detector side I focussed on the heart of the LHCb spectrometer – the Vertex Locator (VELO), a silicon detector from which particles from proton collisions emerge and which is therefore the most damaged by their radiation. The main role of the Vertex Locator (VELO) is to provide track coordinates that will be used for the reconstruction of the production and decay vertices, thus time-life measurements of long-life particles. The measurements need to be precise, so any deviations from the optimal operation parameters should be quickly spotted and fixed. It requires efficient monitoring, especially of the impact of the particle fluence on the detector performance. I am a member of VELO group and I took part in the study of the radiation damage in the silicon VELO sensors, mainly in the monitoring of the leakage current as a function in temperature. I also made a new simulation of particle fluence[2] to be used for the prediction of the evolution of the leakage current and of the effective depletion voltage [1]. These parameters are currently are the most serious consequences of the particle irradiation. My results were discussed and approved by the VELO group, presented on conferences and published [2]. Benefiting from the discussions within the RD50 group [4], which I am also a member, I became an expert on the subject of radiation damage in semiconductor detectors operating in high luminosity experiments and had an honour to report the RD50 achievements and recommendations on four conferences. I was also given the research grant from the National Science Centre (NCN) and plan to continue and extend these activities for the next years of work in the VELO group and for the High Luminosity LHC.

My interest in heavy flavour physics started during my PhD study when I participated in the DELPHI Collaboration at Large Electron-Positron Collider (LEP). Thanks to the silicon Vertex Detector, used on this scale for the first time, the DELPHI detector was able to measure time-life of B mesons and provided the first estimations of the CKM matrix parameters, further studied by the B-factories [5].

---

[1] In the LHC also the beams of heavy ions (Pb) are accelerated.

[2] Fluence ϕ is defined as number of particles incident on a sphere of cross-sectional area a: $\phi = \frac{dN}{da}$ $[cm^{-2}]$. Flux is the number of particles per time unit: $\varphi = \frac{dN}{dt}$ $[s^{-1}]$. Flux is often considered as a *fluence rate*. Fluence is therefore the integral of flux and should be always given with the time period.

After my PhD I joined the LHCb Collaboration, I participated in the simulation of B meson decays and determined the experiment sensitivity to the CKM γ angle. I started the real data analysis as soon as they were available in the year 2010.

I decided to take care of the decay $B_s^0 \to D_s^{\mp} K^{*\pm}$, later also for the decay $B_s^0 \to D_s^{*\mp} K^{*\pm}$, which is currently studied by my student under my supervision. So parallel to my interest in the VELO operation, I become responsible for the preparation of the selection and analyses of the process $B_s^0 \to D_s^{\mp} K^{*\pm}$, never reported before. Due to the high mass of the B_s^0 meson, it was non-accessible in B-factories. I started the study of the generation samples, then participated in the preparation of the simulation and checked the performance of the whole chain of preselection algorithms maintained by the central software of the experiment. I checked the LHCb sensitivity to the CKM γ angle with the use of this process when the sufficient amount of data are available.

The decay of $B_s^0 \to D_s^{\mp} K^{*\pm}$ meson gives six particles in the final state and requires the reconstruction of three decay vertices. Therefore, this not a "first-day measurement" and due to the complicated topology requires large amount of data. The proper VELO performance is here of a crucial meaning. I worked-out the selection criteria that allowed me to select a few thousand of events that are considered as candidates for the observation of this decay. The official results will be published with the use of whole Run I and Run II data. I am the member of the LHCb working group named *B To Open Charm* and showed the LHCb results on this subject on many conferences.

1. LHCb experiment

The LHCb (Large Hadron Collider beauty) experiment is one of the four main experiments that operate at the Large Hadron Collider (LHC) at CERN [6]. The experiment is designed to study *CP* violation, observation of rare decays of beauty and charm particles, and search for New Physics (NP) evidences using indirect measurements. Whereas ATLAS and CMS are general-purpose detector with a broad physics programme spanning from the Standard Model (SM) though supersymmetry (SUSY) to extra dimensions, the LHCb detector is a single-arm forward spectrometer dedicated for studying flavour physics at the LHC. The LHCb programme is thus highly complementary to the direct searches performed at ATLAS and CMS.

The LHCb spectrometer (Fig.1a) is a single-arm forward spectrometer covering the pseudorapidity range $2<\eta<5$. Its forward geometry exploits the dominant heavy flavor production mechanism at the LHC since the $b\bar{b}$ pair production in proton-proton collisions at the LHC is spatially correlated and occurs predominantly at small angles with respect to the beam axis.

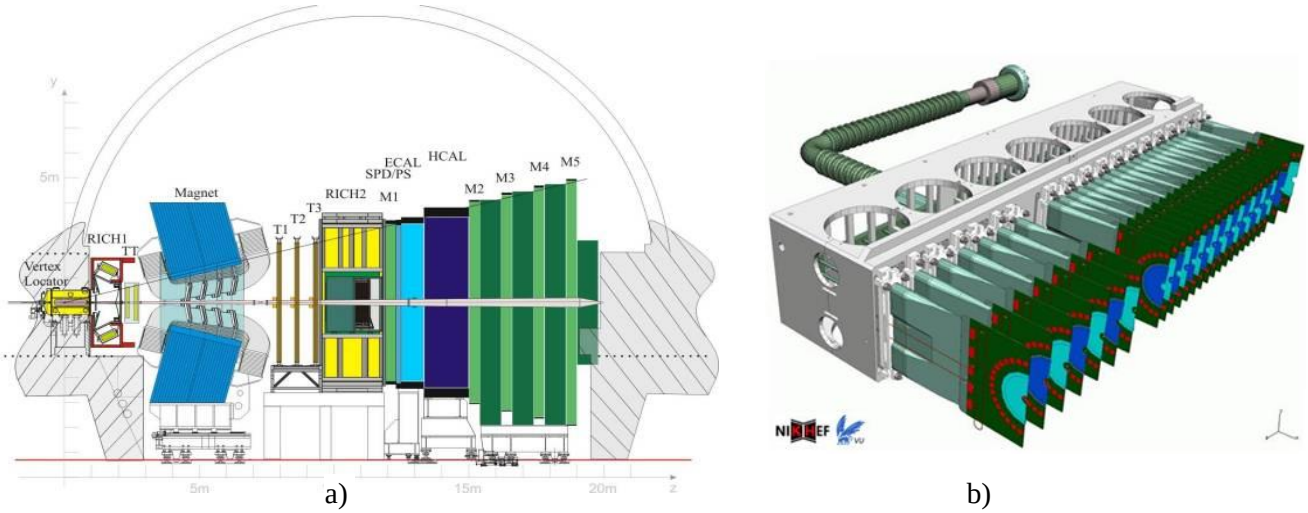

a) b)

Fig. 1. a) View of the LHCb spectrometer. b) The LHCb VELO (one half) [7].

The detector includes a high-precision tracking system consisting of a silicon-strip vertex detector (Vertex Locator) surrounding the proton-proton interaction region, one silicon-strip detector before the magnet (TT), and three tracking stations behind the magnet (T1-T3). The tracking system provides a measurement of charged particle momentum with a relative uncertainty that varies from 0.5% at low momentum to 1.0% at 200 GeV/c. A decay time resolution of about 50 fs is obtained at LHCb thanks to the accurate measurement of production and decay vertices [6].

Two ring-imaging Cherenkov detectors (RICH) provide efficient identification of charged particles with momenta up to 100 GeV/c. Photons, electrons and hadrons are identified by a calorimeter system Muons are detected by a system (M1-M5).

Due to huge number of events produced, an effective on-line event selection is required where the rate is reduced by a first level hardware trigger (L0) and further by two software high level triggers (HLT). This selects interesting events by means of high transverse energy and momentum signatures. The HLT performs a reconstruction of the tracks in the event in real time and runs a mixture of exclusive and inclusive selection algorithms.

The VELO consists of two movable halves that contains 23 modules situated perpendicular to the beam axis, see Fig.1b. All but two modules are double-sided designed to measure r coordinate from one side (R-type sensors) and ϕ (Φ-type sensors) from the other, see (Fig. 2a). Two modules contain only one sensor (R-type) [7]. Modules are placed 7 mm (the active part of the sensor 8.2 mm) from the beam line, what is smaller than the aperture required by the LHC during injection. To avoid the risk of sensor damage by the proton beam, VELO must be retracted up to 30 mm during the beam injection.

2. Radiation damage in the semiconductor VELO LHCb sensors

Majority of the VELO sensors are n+-on-n type, having a row of diodes structured on a single silicon wafer. The heavily doped n+ side in silicon detector plays a role of collecting electrode, whereas bulk of the detector is less-doped n-type silicon, p+ is used as backplane. This kind of structure is depicted in Fig. 2b. Two sensors are n^+-on-p type.

The LHC provides 2808 bunches with more than 10^{11} protons each at nominal conditions. Protons are accelerated up to $\sqrt{s}$ =13 TeV the centre-of-mass energy and collided with a frequency of 40 MHz.

The total cross section for proton-proton interaction at $\sqrt{s}$=8 TeV is $(96.07 \pm 0.18 \pm 0.31)$ mb, out of this 71.5 mb is related to the inelastic processes. Assuming the nominal LHC luminosity to be

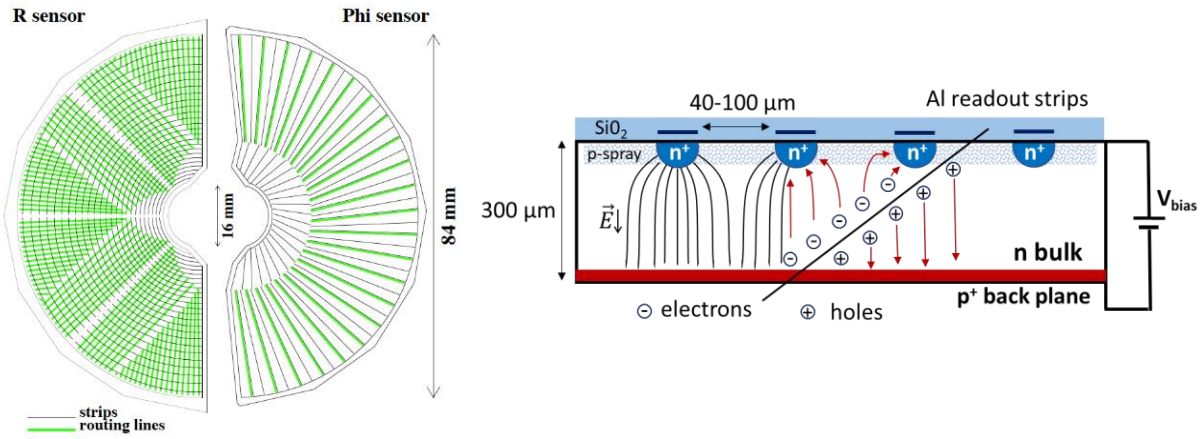

a) b)

Fig. 2. a) The layout of R and Φ sensors. The routing lines in R sensors are perpendicular to the strips, while in Φ they are parallel [7]. b) Cross-section of the n^+-on-n type VELO sensor. A traversing particle loses energy while passing through the sensor and creates electron-hole pairs in the depletion zone. They drift in the electric field towards electrodes inducing signal. Depending of the particle incident angle, the generated charge can be shared between two or more electrodes. Depletion zone extends from the p^+ layer inside the n-type bulk. Lines of the electric field are shown [1].

10^{34} $cm^{-2}s^{-1}$, in each second of running the experiments about $96 \cdot 10^7$ proton-proton interactions occur. Typically, hundreds of particles are produced per one proton-proton interaction with momenta that range over many orders of magnitude.

The LHCb silicon Vertex Locator is positioned closer to the proton beam than any other device operating at LHC (except diamond detectors or scintillators installed to monitor the beam). Therefore, the VELO sensors were irradiated by extremely high fluence of the order of 10^{15} n_{eq}/cm^2 after collecting data that correspond to more than 9 fb^{-1} of integrated luminosity. Currently the LHCb VELO is the most irradiated silicon tracker at LHC.

Particle radiation has permanent consequences regarding the properties of semiconductor detector. Semiconductor devices are affected by two basic radiation damage mechanism: ionization and displacement damage. Charged particles that propagate through the active volume of a silicon sensor lose their energy mainly by ionisation. The generated electron-hole pairs travel through electric field and induce electric signal on electrodes. This process enables the detection of the passing particle. On the other hand, the ionisation causes also considerable damage. Electron-hole pairs are created in insulating layers, like SiO_2 (ionisation energy is $E_i = 18\ eV$). Electrons move quickly to the electrode, but holes move slowly and can be easily trapped in the oxide volume leaving positive charge. This charge creates a parasitic electric field and has impact on the collection of charge carriers. Ionisation damage, however, does not create any crystal defects.

Both charged and neutral particles may also lose their energy through nonionising collision with the lattice atoms (silicon or dopant). The recoil atom, called primary knock on atom (PKA) can migrate through the lattice causing the dislocation of further atoms. The displacement damage results in permanent changes of the semiconductor material.

Displacement damage depends on the nonionizing energy loss (energy and momentum transfer to lattice atoms), which depends on the mass and energy of the impinging particle. The struck silicon atoms that are displaced by interaction with a passing particle may carry energy sufficient to move through the crystal and for further creation of defects, what results with more vacancies and interstitial atoms. All are mobile in the silicon and perform secondary reactions, like combination with each other or with impurities, cluster formation and finally capture or recombination. At room temperature, a major part of the pairs annihilates and do not cause any permanent damage, but the remaining vacancies and interstitials substantially change the electrical properties of the silicon device. The primary defects, silicon interstitials and vacancies, may interact with crystal impurities present in the crystal, or impurities, that became active after radiation. Defect states can act as donors, acceptors (the dominant defect charge states) or can be electrically neutral [9].

A large effort has been made to correlate the macroscopic changes observed in the silicon detector with specific microscopic defects. The radiation induced damage manifests itself in three important ways:

- increase in leakage current, caused by the formation of mid-gap generation and recombination centres which facilitate the transition of electrons from the valence to conductive band. The increase is proportional to particle fluence,
- change the effective doping concentration of the sensor, which has an impact on the on operating voltage needed for total depletion,
- loss of charge collection efficiency due to charge carrier trapping in states close to the band edges. That effect causes the loss of signal and is of the main concern in heavily irradiated sensors.

The impact of radiation damage is not constant after irradiation stops, since the created defects can anneal. Silicon interstitial and vacancies can recombine, stable defects are also able to transform and become inactive, which is beneficial for the sensor performance. Inactive defects can also be reactivated and thus increase the impact of radiation damage again. The rate of damage is strongly dependent on temperature and can be predicted basing on the models, like so-called Hamburg model [9].

What is of major meaning, it that the radiation damage macroscopic effects accumulate over time and in long lasting experiments must be predicted at the design stage, since damaged sensors usually cannot be easily replaced.

2.1 Monitoring of the radiation damage in the VELO sensors

The currents in the VELO sensors are constantly measured and recorded to monitor the change caused either by the radiation damage or other factors (like increase or decrease of high voltage, change of operating temperature, etc.). In addition, two special current-related scans are regularly undertaken: the current dependency on temperature (IT scans) and on voltage (IV scans).

The expected radiation induced increase of leakage current in the bulk of the sensor (normalized to the active detector volume) rises linearly with the equivalent fluence, according to the formula:

$$\Delta I = \alpha \, V_{ol} \, \phi_{eq} \, , \tag{2.1}$$

where α is called the *current related damage rate* or *damage constant*, ϕ_{eq} is the 1 MeV neutron equivalence fluence, i.e. the particle fluence normalised to the fluence of neutron with kinetic energy of 1 MeV

This dependency for the VELO sensors is shown in Fig. 3a. The change in the leakage currents of all VELO sensors are found to evolve proportionally to the delivered luminosity, whereas it is relatively flat during the long breaks between data-taking periods. A typical increase is about 1.9 μA per 0.1 fb^{-1} of the delivered luminosity. The effect of annealing of the currents, is visible, especially during long technical stops.

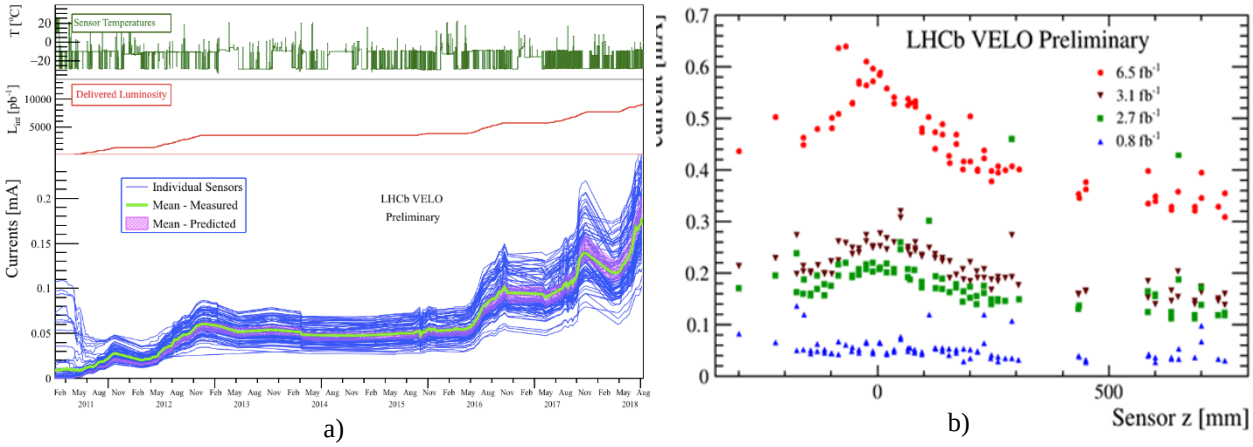

a) b)

Fig. 3. a) Leakage current for the VELO sensors as function of time (bottom), delivered luminosity (middle), and sensor temperatures [3]. Operational VELO temperature is -7°C, but occasional warmings were present. b) Leakage current of the VELO sensors as a function of the sensor position along the beam line. Currents are scaled to 0°C. The three sets of data correspond to the first period of data taking (0.8-3.1 fb^{-1}), whereas the last one (red dots) shows the measurements that were taken during the Run II period, when about 6.5 fb^{-1} of data was delivered to the LHCb spectrometer [1].

During the IT scans the current and temperature were recorded as a function of time. Such tests may be done only during LHC shutdowns, without collisions, when sensors are fully depleted. The temperature was gradually ramped up and down, either with a step of 2 degrees, leaving 10 minutes for stabilisation, or the sensors were warming continuously, starting from the lowest setting point of -28°C up to the 5°C [1].

Basing on IT scans, a comparison of the leakage currents in sensors irradiated with increasing level of fluence can be done. Current measured at different temperatures $I(T)$ are scaled to the same reference temperature 0°C $I(T_R = 0°\mathrm{C})$ using the relation:

$$\frac{I(T_R)}{I(T)} = \left(\frac{T_R}{T}\right)^2 exp\left[-\frac{E_g}{2k}\left(\frac{1}{T_R} - \frac{1}{T}\right)\right].$$

where E_g is the gap energy: $E_g = (1.24 \pm 0.06)$ eV, T- the absolute temperature and k stands for the Boltzmann constant.

In Fig.3b the sensor currents measured during IT scans, scaled to 0°C and averaged, as a function of sensor position are shown [3]. The increase in values is clearly visible. Also, the difference between the current in sensors close and distant to the IP is noticeable, indicating that the sensors were under vitally increasing radiation field even when measurement were done after the same delivered luminosity [3]. The increase of leakage current with the luminosity (and thus particle fluence) is a clear sign of defect creation and radiation damage.

The detectors at the LHC have been irradiated for more than seven years by now, with an 18 months break. Approximately one third of the year the accelerator delivers collisions of the beams of protons, so the sensors are simultaneously irradiated and annealed. The temperature varies between -8°C during data taking and the nominal (in case of LHCb VELO) temperature -28°C during inter-fills and technical stop periods, with a several days per year of accidental or planned warmings. These factors need to be considered in evaluation of the damage constant α [1]. However, basing of IT scans and fluence simulation, the effective damage constant α_{eff} can be determined.

The most irradiated sensors are chosen and current measured in IT scans, calculated for 0°C, is plotted as a function of delivered luminosity and neutron equivalent fluence. The linear function fitted to the measurements provides the value of $\alpha_{eff} = (1.27 \pm 0.4) \cdot 10^{-18}$ A/cm^3 [1]. This value represents the *effective* damage constant that is specific for the VELO sensors and can be compared only with the sensors irradiated and annealed in similar conditions. Currently, the discussion and results presented on RD50 Workshops show that the value of α_{eff} obtained in this analysis is with agreement with other LHC experiments [4].

The bulk generation current is mainly the result of thermal excitation, it varies exponentially with temperature, according to the formula (2.2).

$$I(T) \propto T^2 e^{-\frac{E_{eff}}{2k}T}, \tag{2.2}$$

here E_{eff} is an empirical parameter related to the energy position of a single deep level representing the sum of all current generation centres created in the sensor bulk. The fits to the one of the first IT scans taken after 0.8 fb^{-1} and during Run II after 6.5 fb^{-1} of luminosity were delivered to the experiment are shown in Fig. 4a.

The effective energy gap E_{eff} depends on defect concentration and, since the generation of charge carriers comes mainly from the middle of the gap, it is close to intrinsic silicon energy gap; $E_{eff} \approx E_g$.

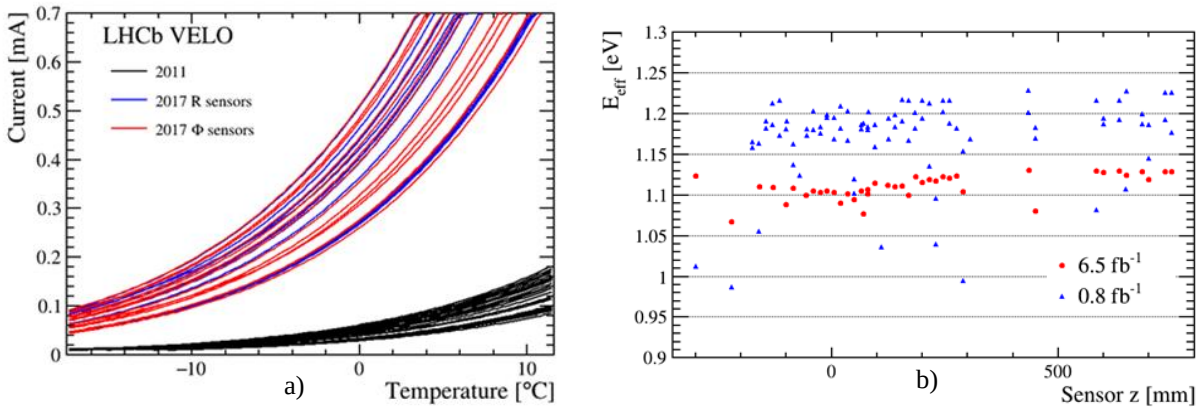

Fig. 4. a) Fits of the leakage currents to the data from IT scans according to the Eq. (2.2). IT scans were taken in 2011 (black lines) and 2017 (red and blue lines) and correspond to the delivered luminosities of 0.8 fb^{-1} and 6.5 fb^{-1} respectively [3]. b) Effective energy gap evaluated for all VELO sensors from the fit to current-temperature dependency as a function of the sensors' position. The data correspond to the light and the most heavily irradiated sensors (0.8 fb^{-1} and 6.5 fb^{-1}) [1].

For the silicon sensors a literature value states: $E_{eff} = (1.214 \pm 0.0014)$ eV [11][10][11]. Measurements of a current as a function of the sensor temperature (IT scans) can be used for determination of E_{eff} after irradiation.

For the purpose of the analysis of the IT scan data a dedicated program was constructed. The two trending: current and temperature were matched to each other extracting the current dependency on temperature. The smart reconstruction method used in the algorithm automatically discovered and rejected the discontinuities in input data.

Effective energy gap E_{eff} was fitted for each sensor using the formula (2.2). In Fig. 4b the E_{eff} as a function of sensor position, determined with data from the beginning of VELO operation and after the 6.5 fb^{-1} of luminosity was delivered to the LHCb, is presented.

For the quantitative description of E_{eff} dependency, the neutron equivalent fluence ϕ_{neq} that every sensor has been irradiated, up to the day of IT scan, is calculated with a FLUKA simulation (see Chapter 2.2). Fluence is calculated taking into account the LHCb delivered luminosity and the proton centre-of-mass-energy $\sqrt{s}$ =7 and 13 TeV. Since the leakage current is measured as an average value for the whole sensor, also the fluence is determined in this way. The average fluence ϕ_{neq} simulated for the VELO sensors and the mean values of E_{eff}, separately for each IT scan, are calculated. It may be noticed that the value of E_{eff} decreases when the sensors are more severe irradiated to the value E_{eff} =1.11 ± 0.001 eV (statistical uncertainties only). This tendency is in agreement with the value obtained in the laboratory conditions [10] and very recent results shown in the RD50 Workshops [4]. This is the first evaluation of E_{eff} for silicon sensors irradiated at LHC.

2.2 Fluence simulation

The study on leakage currents in the VELO sensors, presented in Chapter 2.1 required the knowledge of the particle fluence that hits each of the sensor. For the purpose of this study a simulation tool FLUKA is used [10]. This a diverse software platform that includes generator of collisions, package for geometry description, particle transport and interaction with matter. Several samples of proton-proton collisions at the centre-of-mass energy $\sqrt{s} = 7$ TeV and 13 TeV were generated and beam parameters that are equivalent to the LHC Run I and Run II conditions. The study of two generators (Pythia 8 and DPMJET) of proton -proton collisions at LHC energies was done beforehand. The observed differences between them originated from the different methods used for the hadronisation and different components of the elastic and inelastic cross-sections in the total cross-section. It was noticed that Pythia 8 generator provided about 15-20% more hadrons than DPMJET, depending on the pseudorapidity of particles. This influenced the calculation of the particle fluence in the detector. This problem is currently under discussion among the all LHC experiments since after the upgrade of the experiments.

In the LHC environment, the main source of particle radiation is prompt production of particles in proton-proton collisions. Another source of radiation is the production of secondary particles in the interactions with the detectors and the decay of radionuclides (originated in the material activation processes). The main components of the total prompt particle flux are photons (50%), mostly originating from π^0 decays, and next charged pions (43%), kaons (4%), protons (1.3%) and finally neutrons (1.2%) [1]. The particle fluences (defined as a track-length density) for protons, neutrons, pions and kaons, simulated in FLUKA, are shown in Fig. 5-6.

According to the NIEL hypothesis [8], the displacement damage scales linearly with the kinetic energy that is transferred by the particle to the silicon atom, the primary recoil atom can only be displaced when the imparted energy is more than 25 eV. Since it means that possible damage depends both on the mass and energy of incident particle, it is customary to relate the damage to a reference particle (i.e., 1 MeV neutron). The calculation of the equivalent fluence for protons, neutrons, pions and electrons is done basing on the damage functions. The damage functions are determined experimentally with the measurement of the individual reaction cross section, the energy distribution of recoils produced by that reaction, the probability of ionizing and nonionizing energy loss of the recoils as a function of

impinging particles' kinetic energy [4]. The particle fluence, scaled to 1 MeV neutron, ϕ_{eq}, for each of the VELO sensors, are shown in Fig. 7.

The main result obtained in the presented simulation provides the value of the mean fluence in each sensor, which ranges up to 8.5×10^{13} n_{eq} for 1fb^{-1} at $\sqrt{s}$=7 TeV and 1.1×10^{13} n_{eq} cm^{-2} for 1fb^{-1} at $\sqrt{s}$=13 TeV [1]. According to this simulation, since the start of the experiment up to the end of year 2017, the most irradiated sensor was exposed to about 7.7×10^{13} n_{eq} cm^{-2}. The inner part of this sensor obtained fluence about 46.2×10^{13} n_{eq} cm^{-2} and the most irradiated tip of this sensor 30% more. This gives the value 0.6×10^{15} n_{eq} cm^{-2} what approaches the limit of the Technical Design Report [8].

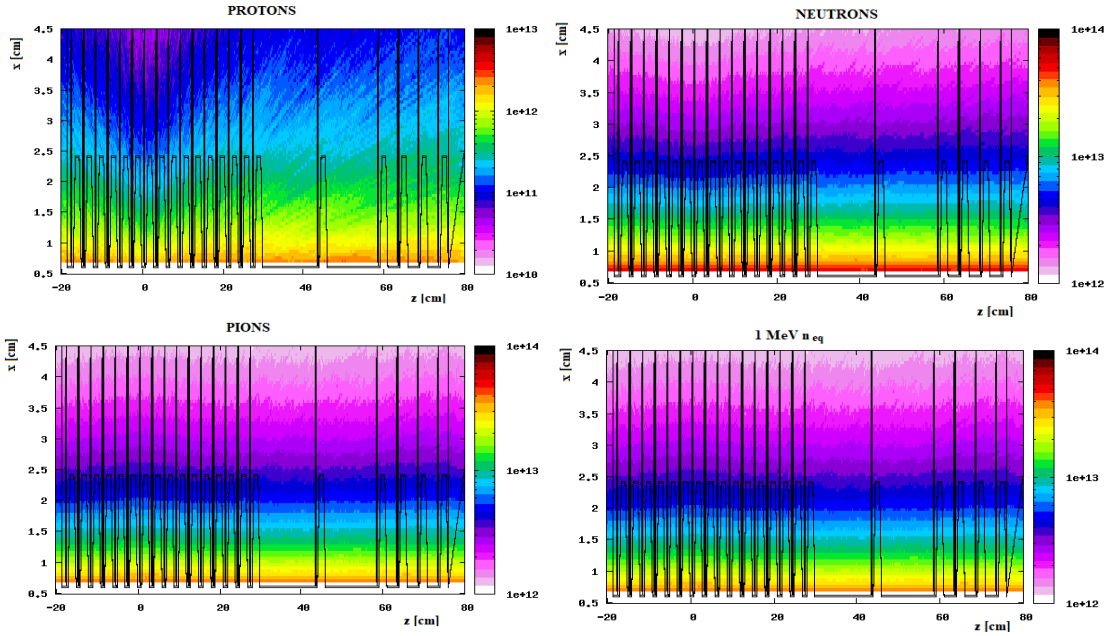

Fig. 5. Fluence of protons, neutrons, pions, and equivalent fluence in VELO sensors, as a function of z positions. Values are scaled to 1 fb^{-1}.

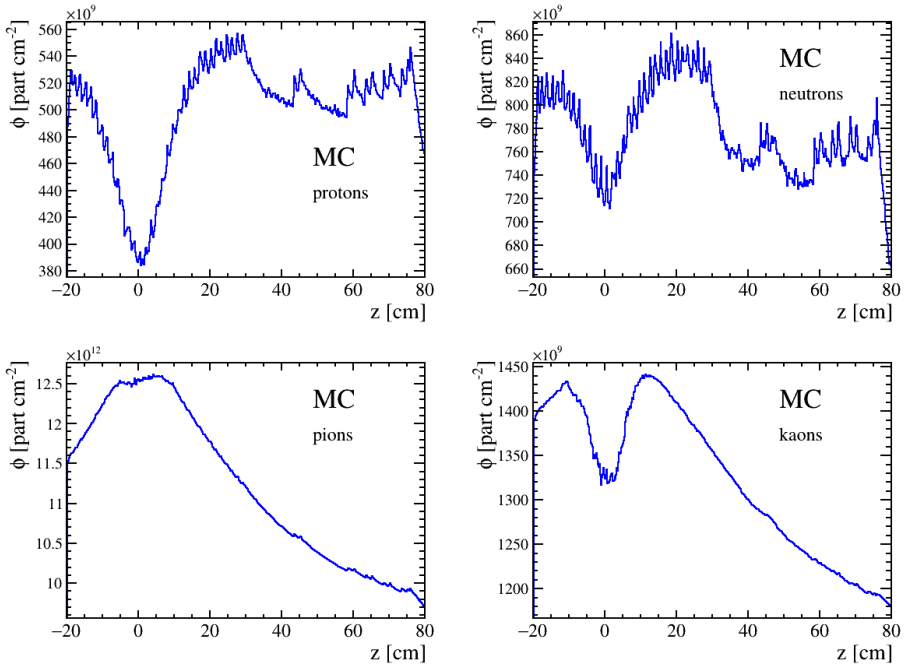

Fig. 6. Fluence of protons, neutrons, pions, and equivalent fluence in VELO sensors, as a function of z positions, averaged over sensor radius. Values are scaled to 1 fb^{-1}.

The particle fluence, simulated with the FLUKA package, although showed a central value that about 15% higher than the result obtained in previous simulation based on Geant4 [6], is in agreement with it, considering the uncertainties originating from the damage function parametrisation. This simu-

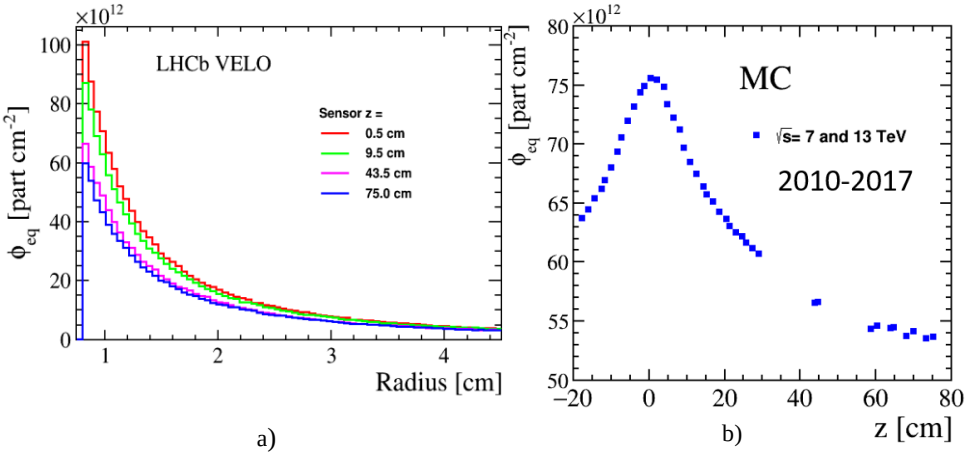

Fig. 7. a) Neutron equivalent fluence as a function of sensor radius $\phi(r)$ for a few representative sensors. Values are scaled to 1 fb^{-1} [2]. b) Simulation of the total neutron equivalent fluence in the VELO sensors that corresponds to the real data taking period 2010-2017 [1].

lation provides the verification of the previous method and shows a new maps of the particle fluence for the VELO sensors. Such a detailed simulation for Run II ($\sqrt{s}$=13 TeV) was done for the first time.

Basing on the results obtained in this study, a prediction for the fluence in the ungraded VELO detector are currently under development. The pixel VELO detector will start to operate in the LHCb spectrometer in the year 2020 (Run III). Sensors will be 5 mm from Interaction Point, and the expected rise of fluence in the inner part of the sensor will be about 40%.

3. Measurement of the Standard Model parameters

The Standard Model (SM) is a quantum field theory (QFT) that describes the spin-1/2 particles (fermions – leptons and quarks), interactions between them via spin-0 bosons exchange (photon, gluons, $W^{\pm}$ and Z^0) and spin-1 Higgs boson responsible for the generation of particles' mass. In QFT physical particles are interpreted as excitation of underlying fields. SM is based on the gauge symmetry group $SU(3)_C \times SU(2)_L \times U(1)_Y$, where $SU(3)_C$ is the symmetry group of strong and $SU(2)_L \times U(1)_Y$ electroweak interaction. The masses of quarks and leptons are generated by the spontaneous symmetry breaking and Higgs mechanism what provides the matrix with the couplings between the quark fields and the Higgs field. Eventually, the unitary Cabbibo-Kobayashi-Maskawa (CKM) matrix is introduced. It acts on the down flavour eigenstates and rotates them into the down weak eigenstates as:

$$\begin{pmatrix} d' \\ s' \\ b' \end{pmatrix} = V_{CKM} \begin{pmatrix} d \\ s \\ b \end{pmatrix}, \qquad V_{CKM} \equiv \begin{pmatrix} V_{ud} & V_{us} & V_{ub} \\ V_{cd} & V_{cs} & V_{cb} \\ V_{td} & V_{ts} & V_{tb} \end{pmatrix}, \tag{4.1}$$

where each element V_{ij} expresses the coupling strength of the weak interaction between the quarks i and j.

The CKM matrix is unitary, therefore we can formulate 12 orthogonality conditions for its complex elements. Three of them are translated into triangles with experimentally accessible sides allowing for the definition of the so-called Unitary Triangle's angles (weak phases) α, β, γ, and β_s.

Since there are no predictions from the SM, all CKM elements must be determined experimentally. The current constrains imposed on the CKM parameters are shown in Fig.8. The results are combinations of many experiments, like B-factories (Belle, BaBar), CDF and LHC experiments (LHCb, CMS, ATLAS) [13]. The triangles are constrained by measurement of their sides and angles, over-constraining helps in spotting the tensions between the measured parameters. The determination of the CKM matrix parameters is regarded as a fundamental test of the unitarity condition, any discrepancy would indicate the phenomena of the physics beyond the Standard Model.

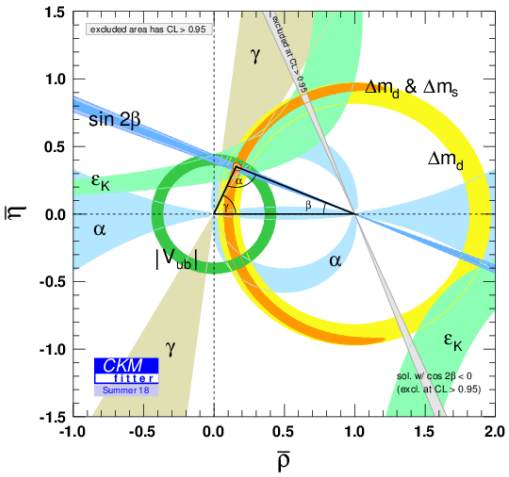

Fig. 8 Experimental constraints of The Unitary Triangle [13].

The violation of discrete symmetries P (parity inversion) and C (charge conjugation) and the combined symmetry CP are fundamental ingredients of the weak interaction visible in the existence of the weak phase in the CKM matrix elements. If CP symmetry was conserved, all elements of the CKM matrix would be real and triangles would be flat. Therefore, the non-zero imaginary part of the V_{CKM} elements is necessary to describe CP violation in the SM. In addition, precise measurements of CP violation and searches for rare decays have a high potential for discovering the effects of New Physics.

Studies of CP violation in heavy flavour physics are amongst the main interests of the LHCb collaboration. They can unveil indirect evidences of New Physics with the energy limits that is not accessible by ATLAS and CMS experiments.

3.1 Potential of $B \to DX$ decays

The rich family of tree-dominated $B \to DX$ decays (customarily named *B to open charm* processes) contains the charm meson in the final state. As a hadron X pion, kaon (also vector particles) or another charm meson are considered. Such decays contain the $b \to c$ transitions together with $b \to u$, thus are sensitive to the CKM angle γ. The achievable precision of the LHCb extends the measurements to higher order processes, also including loop diagrams. CP violation and rare decays are sensitive to new particles and couplings in an indirect way that probes an energy scale beyond the collision energy of the LHC. In case of neutral B mesons, beauty oscillations are possible what opens the possibility for extension of the measurements to the searches for the BSM physics.

3.2 CKM angle γ

One of the core physics goals of the LHCb experiment is to measure the CKM angle γ as precisely as possible. The tree-level processes $B \to DK$ are key measurements in this field. Since in the CKM angle γ definition the top quark does not appear, the precision of predictions, due to lack of the loop diagrams in the first order, may reach far below the current measurement uncertainty. This is to be compared with the B mesons decays to two or three mesons, which include second order loop amplitudes and thus the theoretical predictions are less precise.

There are two methods of the CKM angle γ measurement: time-integrated and time-dependent approach. The former, based on the CP violating observables, was developed in B-factories, exploits the interference from $b \to c$ and $b \to u$ transitions in $B \to Dh$ decays. Here D can be D^0 or $\overline{D}^0$, whereas h stands for $K^{\pm}$, K^{*0} or $\pi^{\pm}$. The interference is ensured when both D^0 and $\overline{D}^0$ decay to the same final state, see Fig.9.

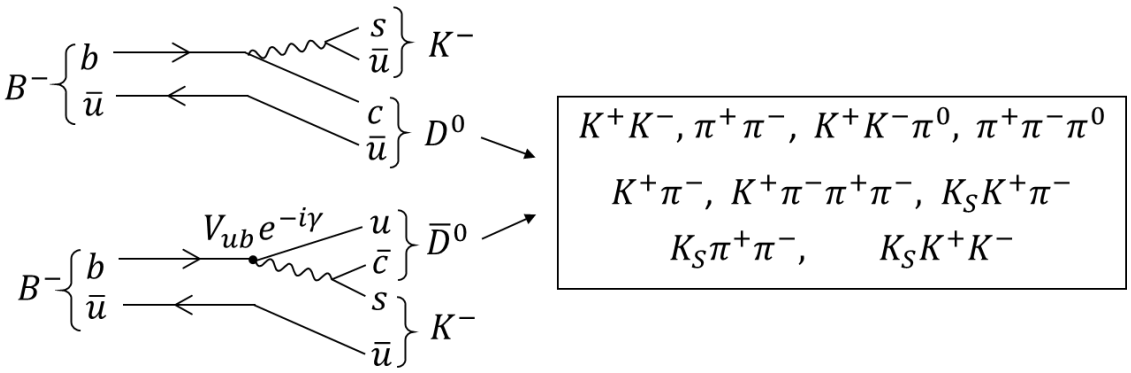

Fig. 9. Diagrams describing the method of the CKM angle γ measurement in time-integrated $B \to DK$ decays. Method is valid for charged and neutral B mesons, the K^{*0} is considered instead of K^- in the former case. The interference is ensured when both D^0 and $\bar{D}^0$ decay to the same final states (as written in the frame).

A different approach is exploited in the study of time-dependent asymmetries in $B^0 \to D^{\pm}\pi^{\mp}$ and $B_s^0 \to D_s^{\pm}K^{\mp}$decays. Also, vector mesons in the final states are to be considered. The principle of time-dependent measurement of the CKM angle γ is shown in Fig.10.

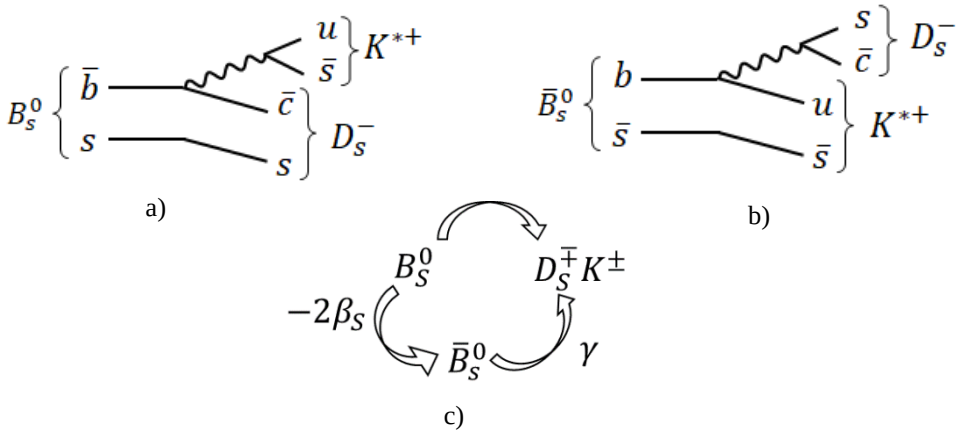

Fig. 10. The Feynman diagrams of: a) $B_s^0 \to D_s^- K^{*+}$, b) $\bar{B}_s^0 \to D_s^- K^{*+}$. Once B_s^0 oscillates into $\bar{B}_s^0$, the transitions $B_s^0 \to D_s^- K^{*+}$ and $B_s^0 \to \bar{B}_s^0 \to D_s^- K^{*+}$ interfere with a result being sensitive to the CKM angle γ. c) Diagram of $B_s^0 \to D_s K$ decays showing the interference between the direct decay of neutral B_s^0 meson and decay after B_s^0 has oscillated into $\bar{B}_s^0$. This interference is sensitive to the phase $(2\beta_s + \gamma)$.

Measurement of *CP* asymmetry in the interference of tree-level $B_s^0 \to D_s^{\mp}K^{\pm}$ (and vector $D_s^{*\mp}K^{*\pm}$ states) processes is sensitive to $(\gamma + \phi_s)$, where ϕ_s describes the $B_s^0 - \bar{B}_s^0$ oscillation $(\phi_s = -2\beta_s)$. Sensitivity to γ comes from the transitions: $\bar{b} \to \bar{c}u\bar{s}$ and $\bar{b} \to \bar{u}c\bar{s}$.

In the decays of $B_s^0 \to D_s^{\mp}K^{\pm}$ two interference amplitudes are of similar size (each decay contains one suppressed and one favoured amplitude) and the effect of interference is enhanced. The CKM angle γ is determined in decay-time-dependent *CP* asymmetries in the decay rates as a function of tagged B decay time. The time-dependent study requires substantial amount of signal events, but it is not model-dependent like time-integrated methods.

The CKM angle γ was already determined in B-factories (Belle and BaBar), CDF, however the current world result is based on the LHCb measurements. Combining all the analyses, γ is constrained as $\gamma = \left(73.5^{+4.2}_{-5.1}\right)^\circ$ [17].

3.3 Analysis of the $B_s^0 \to D_s^{\mp} K^{*\pm}$ decay

During years 2010-2018, the LHCb experiment collected the data that correspond to the integrated luminosity of 9.18 fb^{-1} from the proton-proton collisions at centre-of-mass energy $\sqrt{s}$=7-13 TeV. The cross-section for inelastic processes, in which *b*-mesons are produced, is above 73 mb. The $b\bar{b}$ production cross-section in the pseudorapidity range $2 < \eta < 5$ is $\sigma_{b\bar{b}} = (72.0 \pm 0.3 \pm 6.8)\,\mu b$ and $(154.3 \pm 1.5 \pm 14.3)\,\mu b$ at $\sqrt{s}$=7 TeV and $\sqrt{s}$=13 TeV respectively. It gives roughly $\mathcal{O}(10^9)$ B mesons produced per 1 fb^{-1} and opens the possibility to study B_s^0 decays, unreachable in B-factories. Especially rare, multibody B_s^0 decays are mostly welcome, where the visible Branching Ratio[3] (BR_{vis}) falls below 10^{-6}.

3.3.1 Branching fraction estimation

The branching fraction of the decay $B_s^0 \to D_s^{\mp} K^{*\pm}$ has not been measured yet. It can be estimated taking into account the interplay of strong and weak interaction. The *Effective Field Theory* (EFT) was formulated to disentangle the short- and long-distance QCD effects. An effective weak Hamiltonian for the transition between quarks can be formulated instead of a full QCD Hamiltonian:

$$\mathcal{H}_{eff} = \frac{G_F}{\sqrt{2}} \sum_i V_{CKM}^i \, C_i(\mu) \, Q_i(\mu),$$

The Effective Hamiltonian for $b \to c,u$ or $b \to c,s$ transitions can be written as:

$$\mathcal{H}_{eff} = \frac{G_F}{\sqrt{2}} \left\{ V_{cb}[\, C_1 Q_1^{cb} + \, C_2 Q_2^{cb} \,] + V_{u(s)b}[\, C_1 Q_1^{u(s)b} + \, C_2 Q_2^{u(s)b} \,] \right\},$$

where $Q_1^{qq'}$ describes the weak interactions between quarks, whereas $Q_2^{qq'}$ long-distance strong-interaction effects. The penguin operators are omitted here.

The decay amplitude is expected to factorise into the product of hadronic matrix elements of quark currents:

$$A_{fact} \propto -\frac{G_F}{\sqrt{2}} V_{cb} V_{u(s)b}^* \, c(\mu) \, \langle X|T_A|0\rangle \langle D|T_V|B\rangle$$

where T_A is the amplitude for the creation of a meson X (pion, kaon or any other) from the vacuum via the axial current. This can be parametrised by the respective momentum-dependent decay constant f_π or f_K. The transition matrix element T_V describes the weak $B \to D$ decay, the same as in the semileptonic $B \to Dlv$ decay. The factorisation hypothesis relates the complicated decay amplitudes to the product of meson decay constants and hadronic matrix elements expressed by the semi-leptonic currents. As a result, the transition $B \to D$ is effectively described by the form factor $F_0^{B\to D}$ and the kinematical term $(M_B^2 - M_D^2)$:

$$A_{fact}(B \to DK) = \frac{G_F}{\sqrt{2}} V_{cb} V_{u(s)b}^* \, c f_{\pi,K} (M_B^2 - M_D^2) F_0^{B\to D}\,(m_{\pi,K}^2) \qquad (3.1)$$

The $BR(B_s \to D_s^+ K^{*-})$ prediction might directly be done basing on the formula (3.1), if the decay constant f_{K*} and form factor $F_0^{B_s\to D_s}$ were know. Without these measurements the estimation can be done basing on the available data. Currently it can be achieved by the assumption that ratio of the *BR* of decays to the vector and scalar meson is proportional to the square of the respective decay constants:

$$\frac{BR(B_s^0 \to D_s^+ K^{*-})}{BR(B_s^0 \to D_s^+ K^-)} \propto \left|\frac{f_{K*}}{f_K}\right|^2,$$

[3] Visible Branching Ratio is calculated considering the whole chain of meson decay.

and the ratio $|f_{K*}/f_K|$ should be almost equal to the $|f_\rho/f_\pi|$. Both decay constants f_ρ and f_π are known [17]. Eventually, the $BR(B_s^0 \to D_s^+ K^{*-})$ is estimated taking $BR(B_s^0 \to D_s^+ \rho(770)^-)$, $BR(B_s^0 \to D_s^+ \pi^-)$ and $BR(B_s^0 \to D_s^+ K^-)$ decays into consideration as a ratio:

$$\frac{BR(B_s^0 \to D_s^+ \rho(770)^-)}{BR(B_s^0 \to D_s^+ \pi^-)} = \left|\frac{f_\rho}{f_\pi}\right|^2 \cong \left|\frac{f_{K*}}{f_K}\right|^2.$$

What results in relationship:

$$\frac{BR(B_s^0 \to D_s^\mp K^{*\pm})}{BR(B_s^0 \to D_s^\mp K^\pm)} = \frac{BR(B_s^0 \to D_s^+ \rho(770)^-)}{BR(B_s^0 \to D_s^+ \pi^-)}.$$

providing the result: $BR\left(B_s^0 \to D_s^\mp K^{*\pm}\right) = (5.22 \pm 1.71) \cdot 10^{-4}$ [1].

In this study three-body $D_s^\mp$ final states $K^+K^-\pi^\mp$ are considered and decay $K^{*\pm} \to K_s^0\pi^\pm$ with $K_s^0 \to \pi^+\pi^-$decay. The non-resonant three-body $B_s^0 \to D_s^\mp K_s^0 \pi^\pm$ state is also analysed. BR_{vis} for the decay $B_s^0 \to D_s^\mp K^{*\pm}$ is estimated to be: $(1.07 \pm 0.22) \cdot 10^{-5}$, what results in about 340 ± 65 observed signal events for 1 fb^{-1} of luminosity at proton-proton collisions centre-of-mass energy $\sqrt{s}$=13 TeV and 1‰ of total efficiency [1].

3.3.2 Data selection

The initial selection is performed by LHCb trigger system. At the hardware trigger stage, events are required to have a muon with high transverse momentum (p_T) or a hadron, photon or electron with high transverse energy in the calorimeters. For hadrons, the transverse energy threshold is 3.5 GeV. The software trigger requires a two-, three- or four-track secondary vertex with significant displacement from the primary proton-proton interaction vertices (PV). At least one charged particle must have transverse momentum $p_T > 1.7$ GeV/c^2 and be inconsistent with being produced at the intersection point. A multivariate algorithm is used for the identification of secondary vertices consistent with the decay of a b hadron.

The second stage of the selection (called *stripping*) is performed on data that are accepted by trigger requirements. The recorded events are subjected to preselection criteria that comprises of algorithms grouped in several hundred *stripping lines*. Cuts for the stripping selections are specific for given type of *b*- or *c*- hadron decay and are defined by the user but imposed by central core software. The main aim of the stripping selections is to provide the signal candidates obtained with loose criteria but with retention rate sufficient for data storage. Thus, very general requirements are put for the kinematics and topology of the decay, and very loose particle identification.

Typical topology of a $B \to D^\mp K^{*\pm}$ event is shown in Fig.11. *B* mesons produced in proton-proton interactions at high energies are strongly boosted in *z* direction (along the beam axis). The B_s^0 meson has a life-time of 1.5 ps and can traverse in the spectrometer a few centimetres before decay, so a secondary vertex can be reconstructed directly. The $D_s^\mp$ meson's mean life time is approximately 0.5 ps and a detached vertex can be observed as well.

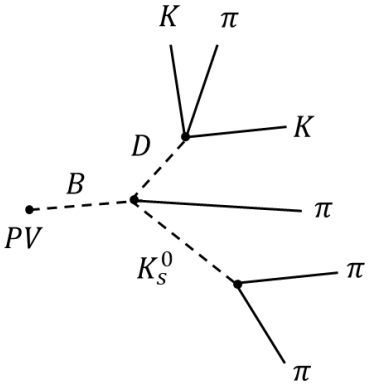

Fig. 11. Topology of $B_{(s)}^0 \to D_{(s)}^\mp K^{*\pm}$ event.

In three-body $D_s^\mp$ final states $K^+K^-\pi^\mp$ resonances can be produced: $D_s^\mp \to \phi\pi^\mp$, $D_s^\mp \to K^{*0}K^\mp$. The $K^{*\pm}$ mesons are reconstructed in the decay $K^{*\pm} \to K_s^0\pi^\pm$, with $K_s^0 \to \pi^+\pi^-$. The non-resonant three-body $B_s^0 \to D_s^\mp K_s^0 \pi^\pm$ state is also considered in this study.

There are six charged hadrons in the final state of the $B_s^0 \to D_s^\mp K^{*\pm}$ decay. The *B* candidate is formed by combining a *D* candidate with a K_s^0 candidate and an additional charged track. *D* candidates

are reconstructed from charge particle tracks originating from a common displaced vertex with the total mass between 1770 and 2070 MeV/c^2 and total transverse momentum greater than 1.8 GeV/c. Momentum of particles from D decay is greater than 5 GeV/c, minimum transverse momentum is 500 MeV/c. Very loose identification criteria are used at this stage.

Tracks should be well reconstructed, vertices separated from one another and well fitted. K_s^0 meson can travel a few centimetres and its reconstruction is performed with separate algorithms. Finally, the sum of transverse momentum of all six particles should be greater than 5 GeV/c, B candidate should have at least 0.2 ps of life-time and its reconstructed momentum should match the direction of flight from the primary vertex to the decay vertex. Due to large $b\bar{b}$ production cross-section, one can expect numerous B_s^0 and B^0 signal candidates fulfilling the stripping selection requirements, together with physical and combinatorial background. Therefore, the further selection criteria are applied after the stripping [1]:

- Preliminary criteria aiming to reduce the data sample size. Very loose kinematical criteria are used. There are neither particle identification nor topological variables used at this stage.
- Multivariate classification to discriminate the $B \to DK_s^0\pi$ signal against the combinatorial background. Mainly variables constraining vertices together with kinematical variables are used.
- Final selection. Tighter pion and kaon identification criteria are applied. Events from mass windows of appropriate intermediate states are chosen for $B \to DK_s^0\pi$ invariant mass plot. Signal candidates for both B^0 and B_s^0 are search for.
- Mass fit. Candidates with masses 5 GeV < $m(DK_s^0\pi^+)$ <5.5 GeV/c2 are used to perform fit to determine the signal yield of B^0 and B_s^0.

The resulting mass distribution are shown in Fig. 12 and 13 [1].

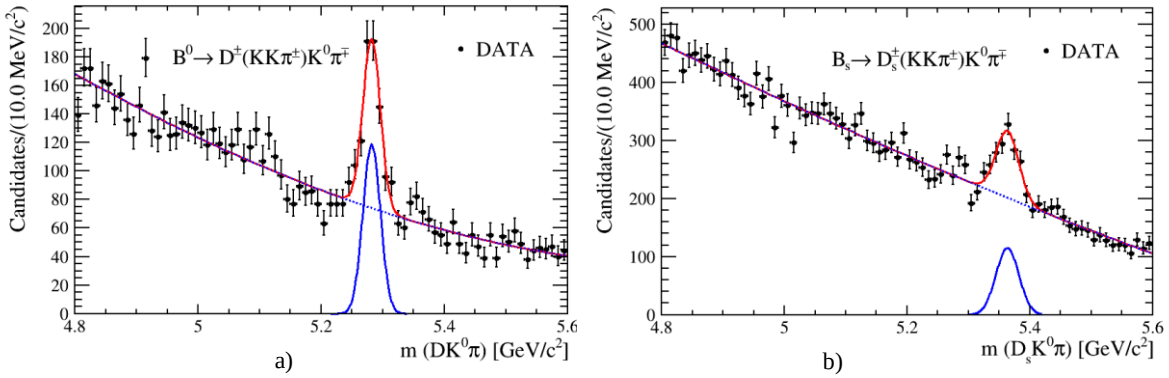

Fig. 12. a) Invariant mass distribution of the candidates $B^0 \to D^-K_s^0\pi^+$ for non-resonant $D^\pm \to K^+K^-\pi^\pm$ decay. b) Invariant mass distribution of the candidates $B_s^0 \to D_s^\mp K_s^0\pi^\pm$ for non-resonant $D_s^\pm \to K^+K^-\pi^\pm$ decay. Both distributions are fitted with Gaussian function for the signal and polynomial for background [1].

3.3.3 Results from the experimental mass fits

Mass plots presented in Figs. 4.4-4.5 allow for the comparison of the B_s^0 signal (where BR is not known) and the B^0 decays, which were measured by BaBar. It should be stressed here that the mass fits were performed basing exclusively on the real data without models supported by Monte Carlo samples. Therefore, the detailed shape of the background is currently not established and will be obtained when appropriate Monte Carlo samples are available. Also, the cross-feed between B^0 and B_s^0 requires additional simulated data.

The number of signal candidates observed in the LHCb data that correspond to the integrated luminosity $\mathcal{L}$, produced with cross-section $\sigma_{b\bar{b}}$ is given by the relationship:

$$N\left(B^0_{(s)} \to D^-_{(s)} K^0_s \pi^+\right) = \mathcal{L}\, \sigma_{b\bar{b}}\, f_{d,s}\, \mathcal{E}\left(B^0_{(s)} \to D^-_{(s)} K^0_s \pi^+\right) \times$$
$$BR\left(B^0_{(s)} \to D^-_{(s)} K^0_s \pi^+\right) BR\left(D^-_{(s)} \to f\right) BR(K^{*\pm} \to K^0_s \pi^\pm), BR(K^0_s \to \pi^+\pi^-), \qquad (3.2)$$

where the $f_{d,s}$ are the probabilities of the s and d quark production respectively (fragmentation fractions) and $\mathcal{E}$ is the total detection efficiency, to be determined in a further study and the BR stands for the branching fractions for the respective decays.

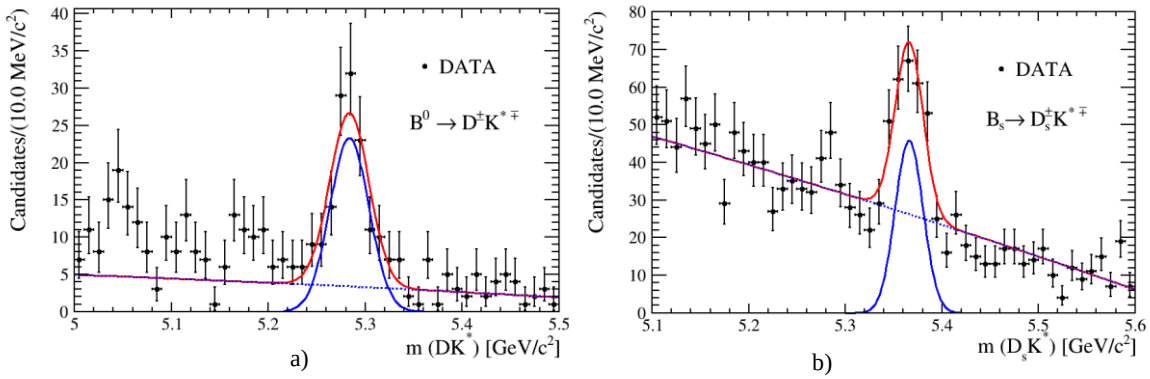

Fig. 13. Invariant mass distribution of the candidates $B^0 \to D^- K^{*+}$ for all $D^\pm \to K^+K^-\pi^\pm$ candidates. b) Invariant mass distribution of the candidates $B^0_s \to D^\mp_s K^{*\pm}$ for all $D^\pm_s \to K^+K^-\pi^\pm$ candidates. Both distributions are fitted with Gaussian function for the signal and polynomial for background [1].

Basing on the fitted signal yields, assuming that, if data involve B^0 and B^0_s decays to the same final state, one can expect similar efficiency in the case of both decays, and considering the branching ratio of the B^0 decay as known, the BR for unknown B^0_s decay can be calculated.

The value of the $BR(B^0_s \to D^+_s K^0 \pi^-)$, estimated according the results of the fit to the mass distributions in Fig. 14-15 and formula (3.2), averaged over three D meson final states, can be expressed as:

$$\frac{N\left(B^0_s \to D^\mp_s K^0_s \pi^\pm, D^+_s \to 2K\pi^+\right)}{N(B^0 \to D^- K^0_s \pi^\pm, D^- \to 2K\pi^-)} = \frac{f_s}{f_d} \frac{BR\left(B^0_s \to D^\mp_s K^0_s \pi^\pm\right) BR(D^+_s \to f)}{BR(B^0 \to D^- K^0_s \pi^+)\, BR(D^- \to f)} \qquad (3.6)$$

and provides the value:

$$BR\left(B^0_s \to D^\mp_s K^0_s \pi^\pm\right) = (5.8 \pm 0.1) \cdot 10^{-4}.$$

The same procedure in case of the $B^0_s \to D^\mp_s K^{*\pm}$ gives:

$$BR\left(B^0_s \to D^\mp_s K^{*\pm}\right) = (4.2 \pm 0.53) \cdot 10^{-4}.$$

The uncertainties are statistical only. The result is in agreement with the prediction based on the amplitude factorisation model.

The additional estimation can be done with the normalisation to the candidates from the favoured decays $B^0 \to D^- K^0_s \pi^+$ and $B^0 \to D^- K^{*+}$, with the D meson decays to $D^+ \to 2\pi K^+$ which are more common than the $D^- \to 2K\pi^-$ thus enables the smaller statistical uncertainties. In this case of a crucial meaning is the determination of the cross-feeds between the $B^0 \to D^- K^0_s \pi^+$, $D^- \to 2K\pi^-, 2\pi K^-$ and $B^0_s \to D^\mp_s K^0_s \pi^\pm$ with the same decay $D^+_s \to 2K\pi^+$. The detailed model of the background must be done in the low-mass region in the distribution of $B^0_s \to D^\mp_s K^0_s \pi^\pm$ with the partially reconstructed decays $B^0 \to D^{*-}(D^-\pi^0, \gamma) K^0_s \pi^\pm$ and $B^0_s \to D^{*\mp}_s \left(D^\mp_s \pi^0, \gamma\right) K^0_s \pi^\pm$. This analysis requires studies on the Monte Carlo samples which be available in the year 2019.

3.3.4 Prospects of $B_s^0 \to D_s^{\mp} K^{*\pm}$ measurements in RUN III

The main aim of this study was to provide selection criteria for the search of the candidates for never previously observed decays $B_s^0 \to D_s^{\mp} K_s^0 \pi^{\pm}$ and $B_s^0 \to D_s^{\mp} K^{*\pm}$. This is the first step towards the estimation of the relevant branching fractions. The first results verified the experiment's sensitivity and shoved the potential of this observation. It, however, also reveals the necessity for the additional studies. It became inevitable to change the preselection condition for the better reconstruction of the vector meson $K^*(892)^{\pm}$. In the current study the decay $K^{*\pm} \to K_s^0 \pi^{\pm}$ is visible but together with the substantial background, probably originating from the random combination of companion pion with the reconstructed K_s^0 vertex. The improvement here will be possible after the refitting of the whole decay tree what can be done in the preselection stage of the analysis. It will be done during the break in data taking period in the years 2019-2020 (LS2).

The plan for the final analysis includes the study of the data from Run I and Run II, i.e. the whole available data collected during the years 2010-2018, what may be possible not sooner than in the 2019 midyear. After applying the worked-out selection criteria, the low-mass side background will be modelled and non-reducible background under the signal mass peak will be statistically subtracted using s$\mathcal{W}$eight technique. This is necessary if reliable time-life distributions are to be obtained for the CKM angle γ measurement. After the signal for $B_s^0 \to D_s^{\mp} K^{*\pm}$ is observed and the BR determined, the decay will be included in the combination with the other LHCb measurements [14]. It will be also possible to use this process for the exclusive determination of the CKM angle γ in the decay-rate analyses of the flavour- tagged B_s^0 events. This is the aim of the Run III studies in 2023, with 50 fb^{-1} of the collected data.

The last but not the least are systematic uncertainties. They have not been studied in detail in this analysis. The effects from the detector itself, tracking algorithms, stripping conditions, and selection criteria influencing the obtained result will be studied based on the Monte Carlo samples or, when possible, will be estimated from the real data.

This analysis proves that the $B_s^0 \to D_s^{\mp} K^{*\pm}$ can be observed in the LHCb detector and shows the feasibility of the BR determination. The next unique result obtained thanks to the observation of the $B_s^0 \to D_s^{\mp} K^{*\pm}$ would be the determination of the CKM angle γ in time-dependent method with a single decay and without the model assumptions in the D meson decays.

Summary

The phenomena of the violation the combined charge-parity (*CP*) symmetry in the weak interaction within the Standard Model was confirmed in the LHCb experiments in heavy hadrons decays. This is a major experiment currently working in the flavour physics field. Due to the subtlety of the observed effects, measuring the *CP* violation parameters requires a significant statistic of events. The LHCb detector is equipped with a precise tracking and vertexing system well-suited to distinguish and identify b- and c-hadron decays. The most apparent evidences of the *CP* violation show up in non-zero measured values of the CKM matrix parameters (phases). On the other hand, if the CKM angles do not sum up into the π value, this will indicate the effects beyond the Standard Model.

The decay $B_s^0 \to D_s^{\mp} K^{*\pm}$ includes the transition from beauty to charm quark through the weak charged current and it should be observed once we consider three-generation structure of the SM and quark transitions with a strength described in the CKM matrix. My study showed one additional confirmation of the SM and the sensitivity to the determination of the CKM angle γ. According to my selection criteria the whole Run I and Run II data will be analysed and eventually the result will be published. This is a realistic scenario since the precision of the measurements of the CKM parameters has increased more than of order of magnitude since the first published result and the average world results are currently dominated by the LHCb measurements.

Nowadays to do research in Particle Physics field one need to build huge experiments and laboratories. For me, the study on the Standard Model cannot not be complete without the knowledge, how the results were obtained. For that reason, during the data taking, I took part in the controlling of the detector operation, assigned to the role of the shift leader or data manager. In addition, I got involved in the monitoring of the VELO subdetector, especially in the radiation damage issues. The first and very clear signal indicating that semiconductor sensors have suffered from the particle radiation is the increase of the leakage current. I've been analysing this growth and also measured the current dependency on temperature. These results were published [2]. In order to connect the observed rise of the leakage current with model of defect creation I made a new simulation of the particle fluence with a detailed map of the flux in the VELO sensors. Since the leakage current has an exponential dependency on temperature with an effective energy gap E_{eff} as a parameter, I could study how it changed while the sensors evidently were getting more and more damaged. Apparently, the electrical structure of the sensors is changed due to the changes made by the created defects and it resulted in the decrease of the E_{eff} [1]. This is the first study of this kind made on a semiconductor device operating in the LHC environment. The results are in agreement with Hamburg model and are used for the design of the new VELO pixel detector that will take data after the LS2, during the Run III of LHC data taking.

References

[1] A. Obłąkowska-Mucha, *Radiation damage in the LHCb Vertex Locator. First observation of $B_s^0 \to D_s^{\mp} K^{*\pm}$ decay*, Wydawnictwo JAK 2018.

[2] A. Obłąkowska-Mucha, Tomasz Szumlak *Optimization of the track fit for the upgraded trigger*, LHCb Note 2016, LHCb-PUB-2014-030; CERN-LHCb-PUB-2014-030.

[3] A. Obłąkowska-Mucha, et al (LHCb VELO group), *Radiation Damage Effects and Operation of the LHCb Vertex Locator*, IEEE Transactions on Nuclear Science, Volume: 65, Issue: 5, 2018.

[4] The RD50 Collaboration - Radiation hard semiconductor devices for very high luminosity colliders, http://rd50.web.cern.ch/rd50/.

[5] J. Abdallah et al., DELPHI Collaboration, *A precise measurement of the B+, B0 and mean b-hadron lifetime with the DELPHI detector at LEPI*, Eur. Phys. J. C33 (2004) 307-324.

[6] LHCb Collaboration, *The LHCb Detector at the LHC*, JINST, 3, (2008) S08005.

[7] R. Aaij, et al. (LHCb VELO Group) *Performance of the LHCb Vertex Locator*, JINST 9 (2014) P09007.

[8] A. Affolder, et al. (LHCb VELO Group) *Radiation damage in the LHCb Vertex Locator*, JINST 8 (2013) P08002.

[9] M. Moll, *Radiation Damage in Silicon Particle Detectors*, PhD Thesis, Universitat Hamburg 1999, DESY-THESIS-1999-040.

[10] Wiehe, S. Wonsak, S. Kuehn,U. Parzefall, G. Casse, *Measurements of the reverse current of highly irradiated silicon sensors to determine the effective energy and current related damage rate*, NIM in Phys. Res. A, vol. 877, pp. 51-55, 2018.

[11] A. Chilingarov, *Generation current temperature scaling*, Tech. Rep. PH-EP-Tech-Note-2013-001, CERN, 2013.

[12] A. Ferrari, P.R. Sala, A. Fasso, and J. Ranft, *FLUKA: a multi-particle transport code* CERN-2005-10 (2005), INFN/TC_05/11, SLAC-R-773.

[13] CKM Fitter, http://ckmfitter.in2p3.fr/.

[14] R. Aaij *et. al., (LHCb Collaboration), Measurement of the CKM angle γ from a combination of LHCb results, JHEP 12 (2016) 087, 1-59,*

[15] A. Obłąkowska-Mucha (on behalf of LHCb Collaboration), *CP-violation measurements in B→DX decays at LHCb*, accepted for publication in Journal of Physics: Conference Series 2018,

[16] M. Neubert, B. Stech, *Non-Leptonic Weak Decays of B Mesons*, CERN-TH/97-99, Adv.Ser.Direct.High Energy Phys.15 (1998) 294-344.

[17] M. Tanabashi et al. (Particle Data Group), Phys. Rev. D 98, (2018) 030001.

[18] B. Aubert et al. (BABAR Collaboration), *Measurements of Branching Fractions and Dalitz Distributions for* $B^0 \to D^{(*)\pm}K^0\pi^{\mp}$, Phys. Rev. Lett. 95 (2005) 171802.

IV. Description of the other scientific achievements

Both my scientific and teaching careers is immanently related to the last years I spend on data analyses and work at the detector.

My first activity as a physicist was connected with DEPHI experiment at LEP. I made my analysis on $\eta_c(2980)$ production in photon-photon interaction. I finished my PhD after the experiment was closed and become a member of the LHCb experiment. Before the onset of data, I made a simulation of the reconstruction of one of the B meson decay and studied experiment's sensitivity to the determination of the CKM γ angle with the use of this process. After the year 2010, during the Run I of the LHC data taking I started to work the VELO group. Since then my working time was divided into B physics analysis, radiation damage study of VELO and teaching at the AGH UST in Kraków. Below, I summarise my achievements, other than monography described in the previous section, divided into three parts that correspond to these fields. The detailed list of my achievements is written down in Supplement 3.

1. B Physics

The LHCb experiment is designed to study heavy flavour physics and rare decays of B mesons. To total number of LHCb published papers on these subjects is above 500. Although I am on the authors' list, I can state that I mainly focused on the analyses of the decays of B mesons to charm mesons and studies of the new reconstruction condition for the detector upgrade. Therefore, I chose 9 publications in which I have a significant contribution:

1. A.Obłąkowska-Mucha (on behalf of LHCb Collaboration), Neutral B-meson mixing and CP Violation at LHCb, Journal of Physics: Conference Series 770 (2016) 012025,
2. Obłąkowska-Mucha, Tomasz Szumlak, Tracking system of the upgraded LHCb, Nucl. Instr. Meth. A 824, (2016) 62-63,
3. Agnieszka Obłąkowska-Mucha (on behalf of LHCb Collaboration), Selected CPV Results from LHCb Run 1 and Prospects for CKM γ Angle Measurements in Run 2, Acta Physica Polonica B47 (2016) 6, 1553-1562,
4. Agnieszka Obłąkowska-Mucha, Recent results from LHCb, Acta Physica Polonica B47 (2016) 2, 245-571,
5. A.Obłąkowska-Mucha et. al., (LHCb Collaboration), Measurement of the CKM angle γ from a combination of LHCb results. JHEP 12 (2016) 087, 1-59,
6. A.Obłąkowska-Mucha et. al., (LHCb Collaboration) Observation of $B^0_s \to D^0K^0_s$ and evidence for $B^0_s \to D^{*0}K^0_s$ decays. Phys. Rev. Lett.116 (2016)161802,
7. A.Obłąkowska-Mucha et. al., (LHCb Collaboration) Measurement of the track reconstruction efficiency at LHCb. JINST 10 (2015) 1-24,
8. A.Obłąkowska-Mucha et. al., (LHCb Collaboration) Measurements of the branching fractions of the decays $B_s^0 \to D^{\pm}_s K^{\pm}$ and $B_s^0 \to D^-_s \pi^+$, JHEP06(2012)115,
9. A.Obłąkowska-Mucha et. al., (LHCb Collaboration) Prospect of the γ CKM angle determination from $B_d^0 \to D^{*\pm} a_1^{\pm}(1260)$ decay process, Acta Physica Polonica B 40(2009)6 1673-1684,

In addition, I participated in 7 conferences in which I was a speaker on the subjects directly connected with my studies. I am a member of the B to Open Charm group and I present my analysis during be-weekly meetings on this group a few times each year. I was (and still I am) an investigator in 3 scientific grants founded by the National Centre of Science (NCN) for my research. I was a member of the organising committee of the LHCb Collaboration Week in 2013, and I plan to be a chairperson of a BEACH conference in Kraków in 2022.

2. Radiation damage

I made an analysis on the leakage currents in the VELO sensors and a new simulation of particle fluence. I am a member of the VELO group and RD50 Collaboration. I have a significant contribution in the following published articles:

1. Agnieszka Obłąkowska-Mucha, et al (LHCb VELO group), Radiation Damage Effects and Operation of the LHCb Vertex Locator, IEEE Transactions on Nuclear Science, Volume: 65, Issue: 5, 2018,
2. A.Obłąkowska-Mucha (on behalf of RD50 Collaboration), Radiation Hard Silicon Particle Detectors for Phase-II LHC Trackers 14th Topical Seminar on Innovative Particle and Radiation Detectors (IPRD16), JINST 12 (2017) C02054, 1-12,
3. Agnieszka Obłąkowska-Mucha (on behalf of RD50 Collaboration), Radiation Damage in Silicon Particle Detectors in High Luminosity Experiments, Acta Physica Polonica B48 (2017) 1707,
4. Agnieszka Obłąkowska-Mucha, Tomasz Szumlak, LHCb Vertex Locator: Performance and Radiation Damage in LHCb Run 1 and Preparation for Run 2, Nucl. Instr. Meth. A824 (2016) 59-61,
5. Agnieszka Obłąkowska-Mucha, et al (on behalf VELO group), The LHCb vertex locator - performance and radiation damage, JINST9 (2014) C01065, 1-11

I have 7 conference presentations connected with the radiation damage and operation of the silicon trackers. I am a leader of the NCN scientific grant, I was a chairperson of the RD50 Workshop in Kraków in the year 2017, I organise simulation sessions of the RD50 Interexperimental workshop at CERN in the year 2018 and the next, 2019.

3. Teaching and popularisation of physics

The experience and knowledge gathered during my work at LHCb allowed me to conduct lectures related to my work (Introduction to Particle Physics and Interactions, Experimental High Energy Physics, CP Violation in Heavy Flavour Physics, Statistics and Data Handling) for undergraduate students at the AGH UST Krakow and organise guided tours in CERN for students and school pupils.
I am a university teacher of the fundamental physics (lectures and tutorials) and Statistics and Data Handling. I have also courses that are directly connected with my scientific career: Particle Physics, CP Violation in heavy flavour physics and Experimental Method for High Energy Physics. Some of my classes are for Erasmus students.

I gave a few lectures on the particle physics for the school pupils, I participated in workshops dedicated to introduction of young people into high energy physics. I was a supervisor of 5 master and 6 bachelor theses, I am currently a subsidiary supervisor of the PhD thesis. I managed to organise a group of highly motivated students working with me on the similar subjects. I also gathered enough experience to conduct new lectures and courses at the AGH UST in Krakow.